FARADAY

Homogeneous and heterogeneous reactions of the *n*-$C_5H_{11}O$, *n*-$C_5H_{10}OH$ and $OOC_5H_{10}OH$ radicals in oxygen. Analytical steady state solution by use of the Laplace transform

Olivier Perrin, Adolphe Heiss, Frédéric Doumenc and Krikor Sahetchian
Laboratoire de Mécanique Physique, CNRS UPRESA 7068, Université P. & M. Curie (Paris 6)
2, Place de la Gare de Ceinture, 78210 Saint-Cyr l'Ecole, France

The different reaction routes of *n*-pentoxy radicals in O_2/N_2 mixtures were investigated in the temperature range 423–523 K under atmospheric pressure. Flow experiments were performed in several reactors, with wall efficiencies increasing from passivated quartz to Pyrex, and with a great variety of mol fractions of O_2 (% of O_2), which was varied from ~0 to 100% O_2; the products, a pentanal-hydroperoxide $C_5H_{10}O_3$ of M_r 118, pentanal, a methylfuranone (γ-valerolactone), pentanol, and three methylfurans were analyzed and identified by GC-MS. Pentanal-hydroperoxide, also called 4-hydroperoxypentanal, $O{=}CH(CH_2)_2CH(OOH)CH_3$, is the major product in passivated quartz vessels. It is formed by two consecutive isomerizations: (i) a fast one, $RO^{\cdot} \rightarrow R_{-H}OH$, *via* a six-membered ring transition state and (ii) a much slower one, involving an $OOR_{-H}OH$ radical, $OOR_{-H}OH \rightarrow HOOR_{-2H}OH$, *via* a seven-membered ring intermediate: $CCCCCO^{\cdot} \xrightarrow{iso} CC^{\cdot}CCCOH \xrightarrow{O_2} CC(OO^{\cdot})CCCOH \xrightarrow{iso} CC(OOH)CCC^{\cdot}OH \xrightarrow{O_2} CC(OOH)CCC{=}O + HO_2$. A chemical mechanism, taking into account all of the experimental results is proposed for reactions of the *n*-pentoxy radical in oxygen. An analytical steady state solution, based on the Laplace transform, has been helpful in rejecting or validating candidate models. Rate constants appearing in the proposed mechanism have been evaluated by the use of an optimization method. This analysis shows that (i) isomerization is the predominant reaction route, accounting for the diversity of end products; (ii) homogeneous pentanal is formed by reaction with O_2 of an isomerized pentoxy radical: $CCCCCO^{\cdot} \xrightarrow{iso} CC^{\cdot}CCCOH \xrightarrow{iso} CCCCC^{\cdot}OH \xrightarrow{O_2} CCCCC{=}O + HO_2$; (iii) methylfurans are also homogeneously produced through an analogous reaction; (iv) γ-valerolactone is formed by a heterogeneous reaction; pentanal and methylfurans are produced in significant quantities through heterogeneous reactions, especially at low concentrations of oxygen (<5% O_2). The implications of heterogeneous reactions of $RO^{\cdot}$ radicals in atmospheric chemistry and in combustion are discussed for those reactions can correspond to a sink for radicals.

Introduction

Anthropogenic emissions play a major role in atmospheric pollution at local and regional levels, not only over large urban areas and industrialized countries, but also on a global scale. The formation of photochemical tropospheric ozone, and other pollutants, is for the most part owing to reactions in which volatile organic compounds (VOCs) and tropospheric NO_x are involved. The VOCs, emitted into the troposphere, originate from ever-increasing road traffic, industrial use of solvents *etc*., and among them ($\geqslant C_4$) species predominate. However, the corresponding chemical mechanisms are uncertain; some questions relevant to the formation of ozone (the level of which is increasing, particularly over Europe) are misunderstood and therefore modelling studies remain unrealistic.

In motor-engine combustion, numerous pollutants are formed near or on the cylinder surface. The formation reactions of those species occur at relatively low temperatures,[1,2] *ca.* 150 to 300 °C. Many of these pollutants would be produced through isomerization reactions of alkoxy[2] radicals $RO^{\cdot}$. These isomerization reactions, which are in competition with decomposition reactions, can occur at temperatures lower than 400 °C and lead to bifunctional compounds such as ketohydroperoxides.[3] It is also known that $RO^{\cdot}$ radicals are key intermediates in the degradation of hydrocarbons (RH) and VOCs, in the atmosphere and/or in combustion, and the relative importance of products is determined by their competing reaction pathways. Reactions of small (C_1–C_3) $RO^{\cdot}$ radicals, methoxy, ethoxy, *i*-propoxy, have been investigated by optical means[4–6] under total pressures of <50 Torr. Only a few products are formed by the two possible pathways, oxidation and decomposition, and these products are easily identified. From a fundamental point of view, Arrhenius parameters need to be better determined, but basic conclusions can be reached as to the importance of oxidation and decomposition, according to temperature and pressure.

Data on compounds with more than three carbon atoms are limited, and often based upon the extrapolation of experimental studies for smaller species. Kinetic data for long chain ($\geqslant C_4$) alkoxy $RO^{\cdot}$ radicals are highly uncertain, although their rate constants and product yields are among the main inputs to be introduced into chemical mechanisms to model the pollution produced during combustion processes and the evolution of atmospheric pollution on an urban, regional and global scale. Intramolecular hydrogen shift-isomerization *via* a six-membered ring has been observed for $RO^{\cdot}$ radicals with four or more carbon atoms in a chain, and accounts for the diversity[7–13] of end products.

Exhaustive reviews, made by Gray *et al*.,[14] and Batt,[15] on the reactions of alkoxy radicals, have covered the literature up to 1986. Many investigations carried out to determine the atmospheric degradation reactions of organic compounds were performed under simulated atmospheric conditions in a variety of environmental chambers.[9–12,16–20] However, owing to the low reaction rates at room temperature, and to observe the products formed, high concentrations of radical precursors were used: for instance, the initial reactant concentrations of species such as HONO, CH_3ONO, NO exceeded that of a real polluted atmosphere by several orders of magnitude.

Therefore, acquired data, although interesting, correspond only partially to atmospheric gas-phase reactions for several reasons: (i) wall reactions[19] and 'background reactivity'[20] and (ii) excessive NO_x concentrations, reducing the reactions in the real atmosphere.

A study involving 2- and 3-hexoxy radicals showed that the 1,5-H shift isomerization could represent by far the main pathway.[9] The gas-phase OH radical-initiated reactions of *n*-pentane and *n*-C_5D_{12} have been investigated by Atkinson *et al.*,[10] and 'NO was included in the reactant mixtures to convert peroxy radicals to alkoxy radicals and to suppress the formation of O_3, and hence of NO_3 radicals.' A C_5-hydroxycarbonyl species, identified by tandem MS, was found to be consistent with a product formed by two successive isomerizations of the 2-pentoxy radical. According to previous results[7,8] and the present work, it might be expected that, in absence of NO, the reaction transforming the radical $CH_3CH(OH)CH_2CH_2CH_2OO^{\cdot}$ into the alkoxy radical $CH_3CH(OH)CH_2CH_2CH_2O^{\cdot}$ would no longer exist, and, therefore, a C_5-hydroperoxycarbonyl compound would be formed instead of the C_5-hydroxycarbonyl species. A similar comment can be made about hydroxycarbonyl products observed from the gas-phase OH radical-initiated reactions of 2,4-dimethylpentan-2-ol and 3,5-dimethylhexan-3-ol.[11]

We previously[7] showed that *n*-butoxy radicals react in oxygen (343–503 K) according to two pathways: 1,5-H-shift isomerization through a six-membered ring transition state forming *n*-C_4H_8OH radicals, $CH_3CH_2CH_2CH_2O^{\cdot} \rightarrow C^{\cdot}H_2CH_2CH_2CH_2OH$, and decomposition, $CH_2CH_2CH_2CH_2O^{\cdot} \rightarrow {}^{\cdot}C_3H_7 + HCHOH$. The difference in activation energies between these two routes (7.7 kcal mol^{-1}) favours isomerization and enabled us to determine the isomerization rate constant of the *n*-butoxy radical, k_{isom} (*n*-C_4H_9O) = $1.3 \times 10^{12} \exp(-9{,}700/RT)$. Homogeneous formation of butyraldehyde occurs mainly from the isomerized radical $C^{\cdot}H_2CH_2CH_2CH_2OH$, through another isomerization, $C^{\cdot}H_2CH_2CH_2CH_2OH \rightarrow CH_2CH_2CH_2C^{\cdot}H_2OH$, followed by the O_2 addition reaction $CH_2CH_2CH_2C^{\cdot}H_2OH + O_2 \rightarrow CH_2CH_2CH_2C{=}O + HO_2$, since (i) the ratio {butyraldehyde/(butyraldehyde + other isomerization products)} is less than 0.3 and independent of oxygen concentration, in the temperature range 448–496 K in passivated quartz reactors, and (ii) the addition of 0–22.5 ppm quantities of NO does not affect the butyraldehyde formation, whereas it lowers the formation of hydroperoxides. The formation of HO_2 was found to be independent of O_2 concentration in the time-dependent study of Mörs *et al.*,[21] which is in agreement with our measurements that show that butyraldehyde formation is independent of O_2.

An unreported peroxide ($C_4H_8O_3$, M_r 104), $O{=}CHCH_2CH_2CH_2OOH$, butanal-hydroperoxide, was shown[7,8] to be the main product. It is formed by the addition of O_2 to the isomerized $C^{\cdot}H_2CH_2CH_2CH_2OH$ radical ($C^{\cdot}H_2CH_2CH_2CH_2OH + O_2 \rightarrow {}^{\cdot}OOCH_2CH_2CH_2CH_2OH$) and subsequent isomerization of the $HORO_2^{\cdot}$ radical through a seven-membered ring transition state, ${}^{\cdot}OOCH_2CH_2CH_2CH_2OH \rightarrow HOOCH_2CH_2CH_2C^{\cdot}HOH$. The rate constant for *n*-${}^{\cdot}OOC_4H_8OH \rightarrow$ *n*-$HOOC_4{}^{\cdot}H_7OH$, $k_{isom(n\text{-}OOC_4H_8OH)} \approx 10^{11} \exp(-17{,}600/RT)$, was estimated, and the consequences for atmospheric pollution drawn. The formation of the above bifunctional peroxide (aldehyde and hydroperoxide) can account for more than 10% of the reactions that consume the $HORO^{\cdot}{}_2$ radical in the atmosphere, at 310 K. Decomposition (by light and/or heat) of this hydroperoxide produces two radicals, and the final result is that one initial radical (*n*-C_4H_9O) is replaced by three. The multiplication of radicals might lead to an increase of tropospheric ozone of several orders of magnitude in *ca.* 10 min; this increase is limited by different types of termination reactions. The successive isomerizations, producing hydroperoxide with M_r 104, grow in importance under low NO concentrations (3 μg m^{-3} in rural areas in comparison with more than 30–60 μg m^{-3} in city areas, whereas the O_3 concentration is about 50–60 μg m^{-3} in rural areas and decreases to 30–40 μg m^{-3} in cities) and at high temperatures, under summer anticyclonic conditions. This process may explain the paradoxical coincidence of high concentrations of tropospheric ozone with low concentrations of NO at the same location.

These experimental[7,8] data were recently confirmed by theoretical calculations,[22] which came to conclusions in agreement with ours, particularly with regard to implications for atmospheric chemistry. The isomerization rate constant for $HOCH_2CH_2CH_2CH(OO^{\cdot})CH_3 \rightarrow HOC^{\cdot}HCH_2CH_2CH(OOH)CH_3$ (k_3) has been determined, in a recent paper,[23] during the thermal decomposition of di-*n*-pentyl peroxide, $H_{11}C_5O\text{-}OC_5H_{11}$, in oxygen and in presence of NO. Isomerization of the $OOR_{-H}OH$ radical (slower than the first one $RO^{\cdot} \rightarrow R_{-H}OH$) occurs *via* a seven-membered ring transition state, and is favoured by the presence of the C–O bond[7,23,24] which weakens the two remaining C–H bonds from their primary *H* value by *ca.* 4 kcal mol^{-1}. It was also established that, in passivated quartz vessels and in the absence of NO, the main compound formed in the gas-phase reactions of *n*-$C_5H_{11}O$ radicals in O_2/N_2 mixtures is the pentanal-hydroperoxide, also called 4-hydroperoxypentanal, $O{=}CH(CH_2)_2CH(OOH)CH_3$ (molecular formula $C_5H_{10}O_3$). Determination of the isomerization rate constant k_3 was made by comparison with the well-known competing reaction $RO_2^{\cdot} + NO \rightarrow RO^{\cdot} + NO_2$ (k_7).

The isomerization rate constant involving the two H atoms of the CH_2–OH group was found, over the temperature range 463–523 K to be

$$k_3 = (6.4 \pm 0.6) \times 10^{10} \times \exp\{-(16\,900 \pm 700)\ \text{cal mol}^{-1}/RT\}\ \text{s}^{-1}$$

and for 1 H atom:

$$k_{3(H)} = (3.2 \pm 0.3) \times 10^{10} \times \exp\{-(16\,900 \pm 700)\ \text{cal mol}^{-1}/RT\}\ \text{s}^{-1}$$

The role of heterogeneous reactions in the formation of end-products was also pointed out:[7] with non-passivated reactors, Pyrex being the most effective, butyraldehyde becomes the main product, in association with low amounts of 2,3-dihydrofuran, a monooxygenated heterocyclic species. Previously, Eberhard *et al.*[9] observed the formation of furanes, hexyl nitrates and other unidentified compounds during a study of the isomerization reactions of 2- and 3-hexoxy radicals in a Teflon chamber. Investigations on the *n*-$C_5H_{11}O$ radical, for which isomerization is expected to play a more significant role, are obviously needed to improve our knowledge on the low temperature combustion and atmospheric degradation of *n*-pentane. We soon noticed the occurrence of homogeneous and heterogeneous reactions for the *n*-pentoxy radical in O_2/N_2 mixtures, and we attempted to understand their role in order to apply this knowledge to atmospheric chemistry and combustion. This is possible if we are able to determine which products are formed in the gas-phase and which are formed heterogeneously, and are also able to determine their kinetic data. To reach this objective, several reactors with different wall efficiencies, and a great variety of O_2/N_2 mixtures, have been used. From the experimental results: (i) an exhaustive formation mechanism of products has been recommended; (ii) a suitable method has been used to optimize the numerical rate constant values at 473 K.

Experimental

Some specific points of the experimental set-up and operating conditions that were previously described,[7] need to be recalled. Di-*n*-pentylperoxide, from which *n*-pentoxy radicals are

generated by pyrolysis (RO—OR → 2RO$^{\cdot}$), was synthesized according to the classical method of Welch *et al.*[25] The vapour of this RO—OR peroxide is entrained in a flow of N_2, and mixed with a flow of O_2; the resulting mixture (O_2/N_2 a few tenths of ppm of di-*n*-pentylperoxide) flows into the reaction vessel, which is located in a thermoregulated oven (±0.5 K). The flows of N_2 and O_2 were measured and electronically regulated by mass flow controllers RDM 280 from l'Air Liquide Alphagaz. Many experiments were carried out under low concentrations of O_2; to maintain an accurate knowledge of the [O_2] an OTO-SX45 mixture of O_2/N_2 (guaranteed molar concentration of O_2 4.51%, supplied also by l'Air Liquide) was used instead of O_2. Flow experiments were performed in several cylindrical reactors in the temperature range 433–523 K under atmospheric pressure. The gas flow was continuously sampled, at the vessel outlet, and the products condensed in a liquid nitrogen trap, for times ranging from 20 to 60 min. When an experiment was stopped, the condensed products were dissolved in (*ca.* 50 μl) methanol or acetonitrile, and (0.5–1 μl) samples were injected (in the split mode, about 1/60 of the sample flowing through the GC column) onto a capillary column, HP-1, 25.0 m × 0.20 mm × 0.50 μm, of a GC-MS Saturn II from Varian; the carrier gas was He 99.9999%, the injector and the transfer line temperatures were 393 K. Two different GC oven temperature programmes were used: (I) from 313 K (4 min), 5 K min^{-1} to 423 K (22 min), and 4 min at 423 K (total time 30 min), (II) from 313 to 363 K in 5 min (10 K min^{-1}), 363 to 373 K in 5 min (2 K min^{-1}), and 373 to 423 K (10 K min^{-1}) (total time 15 min).

To distinguish homogeneous from heterogeneous reactions, four different types of reactors were used: (1) passivated[7] quartz, (2) boric-acid-coated quartz, (3) quartz rinsed with hydrofluoric acid HF and (4) Pyrex glass.

The best reactor, for which passivation of the walls towards radicals is the most effective, is a boric-acid-coated quartz vessel, subsequently treated by the slow reaction of $H_2 + O_2$ (1 : 1) at *ca.* 780 K. If the wall is well conditioned, H_2O_2 is easily produced by the slow reaction of hydrogen. As shown by GC-MS chromatograms, when the passivation began to degrade, the level of hydroperoxypentanal (peaks 11 and 11′) decreased significantly (all other parameters, residence time, temperature *etc.* being maintained equal) whereas that of species such as γ-valerolactone (peak 10) increased. Under good conditions, hydroperoxypentanal is the major product, and is the only one formed entirely in the gas-phase, as shown below. If its formation is reduced, this means that heterogeneous reactions increase to the detriment of homogeneous reactions, and that the passivation has to be updated. When deterioration of wall conditions was observed, a further treatment, by the slow reaction H_2/O_2, was applied, but sometimes the initial state of the wall could not be restored, and the degraded reactor had to be replaced by a new one.

Results

Analysis of compounds

The GC-MS chromatogram displayed in Fig. 1 shows the products generated in an experiment carried out at 483 K in a passivated quartz reactor (mixture O_2/N_2, 1 : 1, residence time 13 s). The following list summarizes (total ion current TIC, electron impact, EI, *versus* time in s) the species observed in order of elution, retention time (GC oven temperature programme I applied), formula and M_r: (1) 157 s, 2,3-dihydrofuran, C_4H_6O, M_r 70; (2) 161 s, butanal $CH_3CH_2CH_2CHO$, C_4H_8O, M_r 72; (3) 165 s, butan-2-one $CH_3COCH_2CH_3$, C_4H_8O, M_r 72; (4) 180 s, 2-methylfuran, C_5H_6O, M_r 82; (5) 201 s, 2,3-dihydro-5-methylfuran, C_5H_8O, M_r 84; (6) 264 s, tetrahydro-2-methylfuran, $C_5H_{10}O$, M_r 86; (7) 294 s, pentanal $CH_3CH_2CH_2CH_2CHO$, $C_5H_{10}O$, M_r 86; (8) 454 s, pentan-1-ol $CH_3CH_2CH_2CH_2CH_2OH$, $C_5H_{12}O$, M_r 88; (9) 600 s, 4-oxopentanal $H_3COCH_2CH_2CH_2CHO$, $C_5H_8O_2$, M_r 100; (10) 800 s, 2-(3*H*)-dihydro-5-methylfuranone (γ-valerolactone), $C_5H_8O_2$, M_r 100; (11) 870 s, hydroperoxypentanal, $C_5H_{10}O_3$, M_r 118; (11′) 970 s, hydroperoxypentanal, $C_5H_{10}O_3$, M_r 118. 4-Hydroperoxypentanal, which can also be called pentanal-hydroperoxide or oxohydroperoxide, elutes after a long time (*ca.* 100 s) and always exhibits the same mass spectrum. The unconsumed di-*n*-pentyl peroxide, $CH_3(CH_2)_4O$–$O(CH_2)_4CH_3$, $C_{10}H_{22}O_2$, M_r 146, elutes only at 1370 s and is not shown on the various chromatograms.

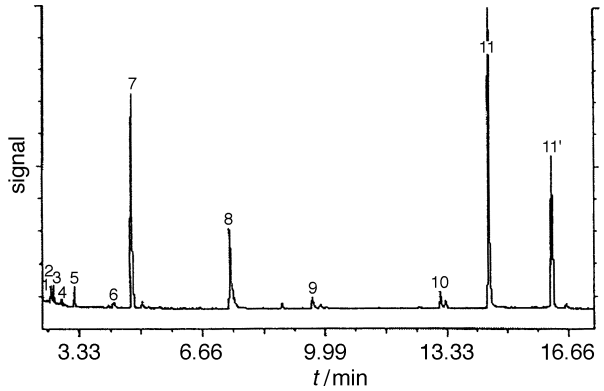

Fig. 1 GC-MS (EI) chromatogram of products obtained with a passivated quartz reactor, ϕ_i = 16 mm, residence time 13 s, 483 K

The identification of each species was performed, as previously,[7] by computer comparison between their EI mass spectrum with the NIST 92 library and subsequent purchase of the library recommended compound which was then injected under identical chromatographic conditions; if the retention time and mass spectrum were the same as the product, positive identification was achieved. Chemical ionization CI mass spectra were also often used to ensure identification of the molecular peak of the investigated product. For unreported species, such as peaks 11 and 11′, a specific and detailed study[23] was carried out, by GC-MS and GC-MS-MS [EI and NH_3 chemical ionization CI conditions]. After micropreparative GC separation of this peroxide was performed, ^{1}H NMR spectra were also acquired. They established the structure of two cyclic isomers, (3*S**,6*S**)-3α-hydroxy-6-methyl-1,2-dioxane and (3*R**,6*S**)-3α-hydroxy-6-methyl-1,2-dioxane. The 4-hydroperoxypentanal OHC–$(CH_2)_2$–CH(OOH)–CH_3 is very likely formed in the gas phase and is in equilibrium with these two cyclic epimers, which are predominant in the liquid phase at room temperature.[23]

Influence of wall conditions

Experiments carried out at the same temperature, 483 K, with the same mixture of O_2/N_2, 1 : 1, and residence times 11–13 s, gave rise to less or more products (in variety and in quantity) depending upon the nature of walls. In Fig. 1–4 are, respectively, displayed GC-MS chromatograms of products formed in (chromatographic peaks are normalized with respect to the highest one): (1) a passivated quartz reactor (inner diameter, id, 16 mm, residence time 13 s, boric acid coating and treatment by the slow reaction, H_2/O_2, at 780 K); (2) the same quartz reactor (id 16 mm, residence time 13 s), but with a degraded passivation; (3) a quartz reactor (id 10 mm, residence time 11 s, rinsed with HF and washed with deionized water and ethanol); and (4) a Pyrex reactor (id 10 mm, residence time 11 s, rinsed with HF and washed with deionized water and ethanol).

It can be noticed that the complexity and number of products formed increase on going from a Pyrex reactor, Fig. 4, (for which heterogeneous reactions are enhanced) to a passivated quartz reactor, Fig. 1, where heterogeneous reactions

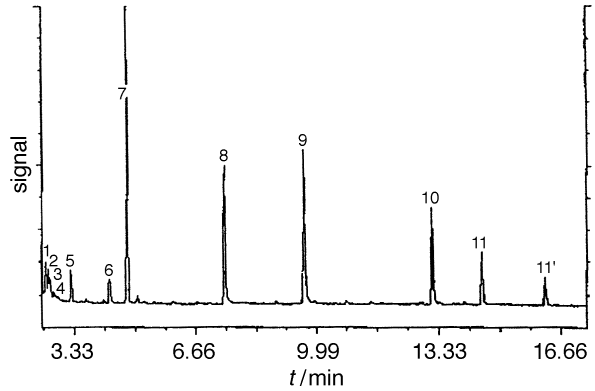

Fig. 2 GC-MS (EI) chromatogram of products obtained with a quartz reactor with degraded passivation, $\phi_i = 16$ mm, residence time 13 s, 483 K

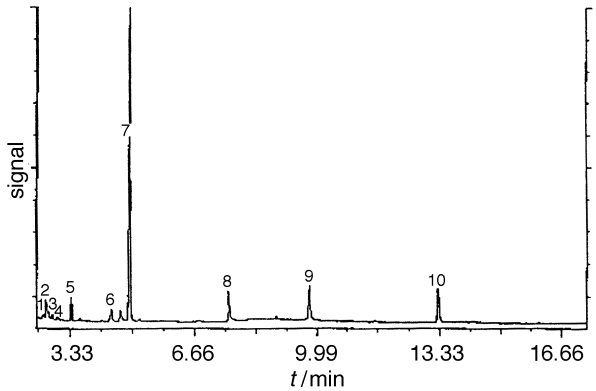

Fig. 3 GC-MS (EI) chromatogram of products obtained with a quartz reactor rinsed with HF, $\phi_i = 10$ mm, residence time 11 s, 483 K

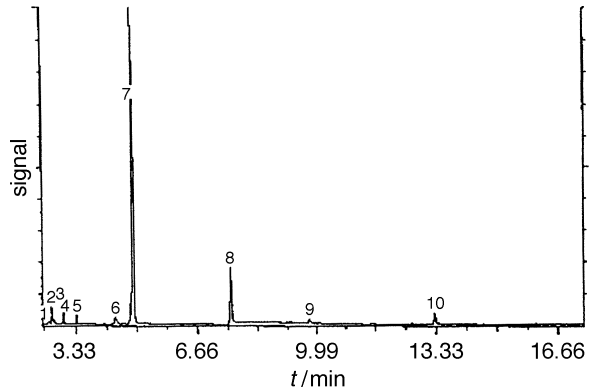

Fig. 4 GC-MS (EI) chromatogram of products obtained with a Pyrex reactor, $\phi_i = 10$ mm, residence time 11 s, 483 K

are minimized and, on the contrary, gas-phase reactions are largely predominant. Hydroperoxypentanal (peaks 11 and 11′) is the major product (70% of the products formed), whereas the pentanal percentage is 23%. The other products represent only a low percentage, methylfurans (peaks 4, 5 and 6), oxopentanal (peak 9), γ-valerolactone (peak 10), or C_4-species issued from decomposition (peaks 1–3).

By comparison to the reference chromatogram of Fig. 1, it can be noted that, with degraded passivation (Fig. 2), heterogeneous reactions increase, but gas-phase reactions remain important: pentanal (7), 4-oxopentanal (9), and γ-valerolactone (10) increase, whereas hydroperoxypentanal (11, 11′) decreases a great deal. Table 1 summarizes data obtained with four types of wall; the observed effects are spectacular. From these results and our previous study on *n*-butoxy[7] radicals, an analogy can be made between the formation of butyrolactone ($C_4H_6O_2$) and that of γ-valerolactone ($C_5H_8O_2$), O-heterocyclic species that differ by a CH_2 group. In each case, the lactone is produced through a heterogeneous process from an $HORO^{\cdot}_2$ radical.

Comparison of the product formed only in the gas phase (hydroperoxypentanal) with that formed heterogeneously (γ-valerolactone), or of species formed at the same time in the gas phase and heterogeneously (pentanal and 2,3-dihydro-5-methylfuran) shows an increase of the various ratios (γ-valerolactone/hydroperoxypentanal), (pentanal/hydroperoxypentanal) and (2,3-dihydro-5-methylfuran/hydroperoxypentanal) with increasing activity of the walls. It can be asserted that hydroperoxypentanal can only be formed in the gas phase: its level is a maximum with passivated walls, decreasing dramatically with more active walls; for decreasing levels of the hydroperoxide, increasing levels of the lactone are observed, and *vice versa*. The lactone and the hydroperoxide are formed from the same $HORO_2^{\cdot}$ radical. The concentration of 4-oxopentanal also increases when wall passivation deteriorates, but it seems that this aldehyde-ketone is formed through heterogeneous decomposition of the hydroperoxide.

Pentanal seems to be generated both in the gas phase and on the walls, because the greater the effect of the walls the more pentanal becomes important until it is almost the sole product in the case of Pyrex. This is proof of a heterogeneous pathway. However, pentanal is also formed in the gas phase after isomerization, according to a mechanism we first pointed out for butanal, in the *n*-butoxy/O_2 system; butanal was formed through the following sequence: $CCCCO^{\cdot} \rightarrow C^{\cdot}CCCOH \rightarrow CCCC^{\cdot}OH$, and $CCCC^{\cdot}OH + O_2 \rightarrow CCCC{=}O + HO_2$. It will be demonstrated below (Reaction mechanism set-up: mathematical study) that pentanal formation occurs after isomerization. It will also be shown that, at a high enough concentration of O_2 (5–100% of O_2), pentanal formation is independent of O_2, whereas at low $[O_2]$ (*ca.* 0–5%) the aldehyde level rises owing to the heterogeneous route.

The three methylfurans formed are mainly heterogeneously generated because their concentration grows with wall effi-

Table 1 Evolution of the percentage of products as a function of the reactor wall

species	passivated reactor (Fig. 1)	'degraded' reactor (Fig. 2)	'HF' reactor (Fig. 3)	Pyrex reactor (Fig. 4)
hydroperoxypentanal (%) peaks (11 and 11′)	70	12.6	0	0
pentanal (%) peak (7)	23	36.7	72.7	93.5
γ-valerolactone (%) peak (10)	2.5	19.2	11.8	3.6
oxopentanal (%) peak (9)	1.8	28.2	1.1	1.3
methyldihydrofuran (%) peak (5)	1.7	3.2	4.3	1.5

ciency (towards destruction of radicals). The most impressive effect is observed for 2,3-dihydro-5-methylfuran (peak 5), which becomes the main product in the very low O_2 concentration range (*ca.* 0–1%). It will be shown later that a homogeneous reaction with O_2 also contributes to the formation of methylfurans.

The results obtained with a Pyrex reactor (id 10 mm) seem surprising, but are in agreement with similar observations made with the *n*-butoxy/O_2 system. The initial peroxide RO–OR, from which RO$^{\cdot}$ radicals are created, must always be decomposed to the same extent in various reactors if the experimental conditions, temperature and residence time, are the same. In fact, with Pyrex, RO—OR is entirely consumed; thus, we have to assume that this decomposition partly occurs on the surface, producing directly pentanal without the intermediate of a radical reaction. Therefore, investigations in Pyrex vessels must be carefully interpreted.

Under conditions favourable to gas-phase reactions only two products predominate: the oxohydroperoxide and the aldehyde; products formed by heterogeneous reactions are also present but only in low concentrations. In contrast, if the reactor walls were very active many different species arise: furans, lactone, aldehyde, aldehyde–ketone, *etc.* To sum up, investigations upon wall conditions enabled us to understand which products are formed in the gas phase and which products are generated on the surface. However, the investigations were not sufficient to determine the *n*-pentoxy/O_2 chemical mechanism, but this gap has been filled by performing studies as a function [O_2].

Investigations as a function of oxygen concentration

The multiplicity of products, as well as the relative ratios between these products as a function of the nature of the wall, reveals the coexistence of homogeneous and heterogeneous reactions. If, indeed, only homogeneous reactions or only heterogeneous reactions were to occur, the observed products would be the same in each case. The products are formed mainly *via* various radical intermediates. The evolution of each of these radicals will enable us to: (i) set up the chemical mechanism of reaction of *n*-pentoxy radicals in oxygen, by following the sequence of successive reactions and (ii) show precisely the formation of the different species.

Whereas the starting RO$^{\cdot}$ radical contains one oxygen atom, it predominantly produces (passivated reactor, O_2/N_2 mixtures) species with three O atoms, hydroperoxypentanal $C_5H_{10}O_3$, and also low concentrations of species with two O atoms, $C_5H_8O_2$ γ-valerolactone and 4-oxopentanal. As molecular oxygen intervenes at several points in the chemical mechanism of *n*-pentoxy radicals, a detailed study employing various [O_2] was needed to identify the oxygen-dependent reaction pathways. When experiments are carried out under very low [O_2], homogeneous reactions with oxygen are disadvantaged to the benefit of heterogeneous reactions. This was another reason to undertake investigations under oxygen with a mol fraction [O_2]/([O_2] + [N_2]) ranging from ≈0 to 100% of O_2.

Fig. 5–8 display GC-MS (EI) chromatograms of species (peak numbering is the same) formed during experiments carried out in the same passivated quartz reactor, id 16 mm, residence time *ca.* 35 s, at 463 K, under decreasing oxygen percentages of, respectively, 42.9, 4.51, 1.29 and 0.45%. With decreasing [O_2], particularly in the range ≈0–5%, it can be noticed that: (i) the 2,3-dihydro-5-methylfuran (peak 5) increases continuously until it becomes the main peak, (ii) the concentrations of polyoxygenated species decrease, especially hydroperoxypentanal (11 and 11′) but also 4-oxopentanal (9), and γ-valerolactone (10).

At 473 K, a series of experiments were performed in the same quartz passivated reactor (id 16 mm) and with the same overall flow of 120 ml min^{-1}, which gave a residence time

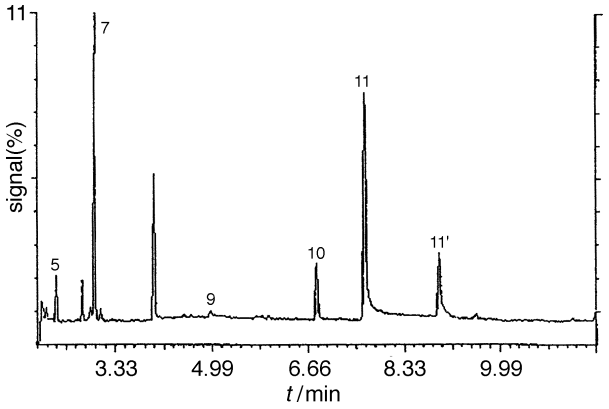

Fig. 5 GC-MS (EI) chromatogram of products obtained with 42.9% O_2, 463 K

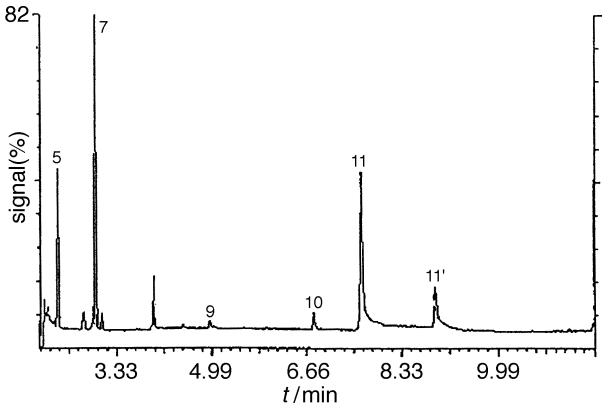

Fig. 6 GC-MS (EI) chromatogram of products obtained with 4.51% O_2, 463 K

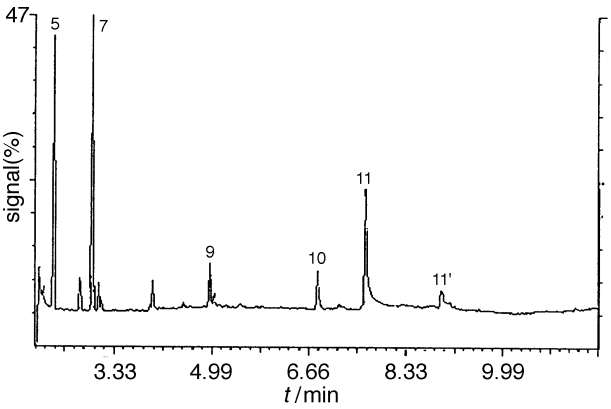

Fig. 7 GC-MS (EI) chromatogram of products obtained with 1.29% O_2, 463 K

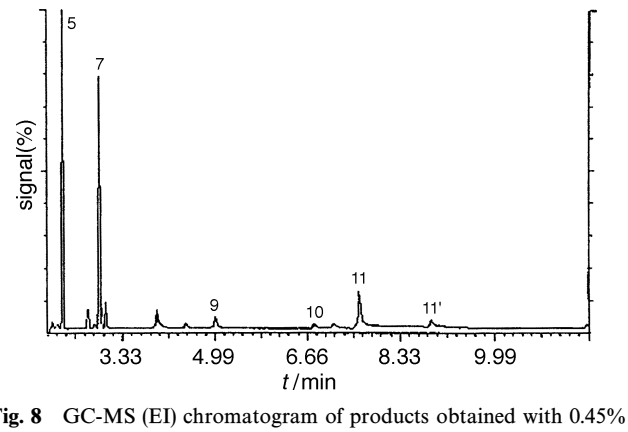

Fig. 8 GC-MS (EI) chromatogram of products obtained with 0.45% O_2, 463 K

$\tau = 26$ s. We investigated the evolution of products *versus* $[O_2]$. In Fig. 9, 12 and 13 are displayed, respectively, plots representing the ratios (pentanal/hydroperoxypentanal), (2,3-dihydro-5-methylfuran/hydroperoxypentanal) and (γ-valerolactone/hydroperoxypentanal) *versus* O_2; it can be observed that these curves increase steeply when O_2 decreases (<10% O_2). These results were systematically analyzed to establish all the formation pathways of end products and to build up the chemical mechanism. For γ-valerolactone and hydroperoxypentanal we can already choose their formation reactions, without the need of a mathematical solution, since their formation can only occur through the intermediate of the $OOR_{-H}OH$ radical.

Formation of γ-valerolactone and hydroperoxypentanal

4-Oxopentanal is assumed to be formed through heterogeneous decomposition of the oxohydroperoxide. The oxopentanal concentration was observed to be always much lower than that of the oxohydroperoxide, because gas-phase reactions are favoured (passivated vessel and the presence of O_2). Therefore, if $[O_2]$ is less than a few %, formation of the oxohydroperoxide is lowered and that of oxopentanal still much more so. Accordingly, the oxopentanal concentration can be neglected before that of the hydroperoxide. It was also noted that, for long residence times, when the initial peroxide RO–OR is practically consumed, the γ-valerolactone concentration does not change, that of hydroperoxypentanal decreases whereas [4-oxopentanal] increases, when the concentration of all other products remains unchanged.

To check the assumption that γ-valerolactone and hydroperoxypentanal are produced from the same radical, the ratio (γ-valerolactone/hydroperoxypentanal) was investigated as a function of the percentage of O_2. A series of experiments were performed at 473 K, $\tau = 26$ s; at low $[O_2]$, the OTO-SX45 mixture of O_2/N_2 (molar concentration of $O_2 = 4.51\%$) was substituted for O_2.

A plot of the ratio (γ-valerolactone/hydroperoxypentanal) against $[O_2]$, (Fig. 13) can be split into two parts: one at high $[O_2]$ (from 10 to 100% of O_2), and a second one of low $[O_2]$ (from 10 to ≈0% of O_2). The ratio is practically constant in the high concentration range, which means that the corresponding ratio of rate constants is independent of O_2. This is in agreement with our assumption, as shown by the reaction sequence shown in Scheme 1.

The *n*-pentoxy radical undergoes a fast isomerization (1, −1), giving the isomerized radical $CH_3C^{\bullet}HCH_2CH_2CH_2OH$ (through the intermediate of a six-membered ring transition state), which is followed by an addition of oxygen. The so-formed $CH_3C(OO^{\bullet})HCH_2CH_2CH_2OH$ radical can react according to two pathways: either a second isomerization, leading finally to the major product, the oxohydroperoxide, or a heterogeneous reaction producing an O-heterocyclic species,

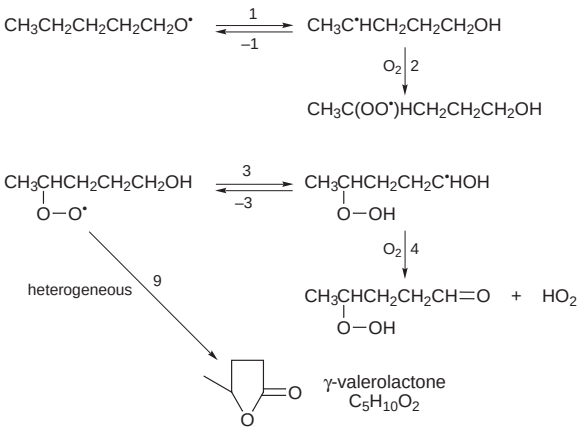

Scheme 1

the γ-valerolactone. In agreement with the above reaction scheme, the ratio γ-valerolactone/hydroperoxypentanal is of zero order with respect to oxygen.

At low percentages of oxygen, reaction (4) becomes the rate-limiting step in the formation of hydroperoxypentanal. Consequently, $CH_3C(OOH)HCH_2CH_2C^{\bullet}HOH$ radicals increase, and as the second isomerization (3, −3) is reversible, in the end, more $CH_3C(OO^{\bullet})HCH_2CH_2CH_2OH$ radicals are present, which enhances the formation of γ-valerolactone to the detriment of hydroperoxypentanal. It can also be noted that the reverse reaction (−2) can be neglected as its activation energy is *ca.* 30 kcal mol^{-1}. To simplify, it can be considered that at low O_2 percentages, the formation of the lactone is favoured because that of the hydroperoxide becomes slower.

The value of k_9, reported in Table 3 has been evaluated from the γ-valerolactone/hydroperoxypentanal ratio at high O_2 concentration (≥10% of O_2).

Reaction mechanism set-up: mathematical study

Methodology

Our purpose is twofold: it consists in building up the reaction mechanism and at the same time evaluating the rate constants involved in this mechanism. The following methodology has been used. We first define all the different possible pathways leading to the formation of a given species. These different pathways are systematically investigated. Each model is mathematically expressed by a set of linear first-order differential equations. Next, the analytical solution of each set of equations is looked for, and an expression of the evolution with O_2 of the concentration ratios of reaction products is deduced, the ratios which have been experimentally determined (the resolution is carried out by the Laplace transform method, with the stationary state approximation). The interest in an analytical solution lies in the fact that it becomes possible to make predictions from that model, particularly about the behaviour of functions, without introducing numerical values of the rate constants (numerical resolution requires, indeed, numerical values). If the function study reveals discrepancies that are found to be unacceptable between the results of the model and the experiments, the assumption was then rejected. In the contrary case, we go to the next step, which is the identification of the rate constants appearing in the provisionally retained model, through an optimization method. If the identification leads to physically unrealistic values of the rate constants, the model is then rejected. In the opposite case, it is considered as plausible. The model we are proposing at the end of this paper has been chosen from those which, at the stage of optimization, succeeded by giving a faithful description of the experimental results, from values of rate constants considered to be realistic. The results obtained from numerical simulation are displayed.

Homogeneous formation mechanism of pentanal

In the gas phase, pentanal can be generated in the presence of O_2 according to two routes: either from the initial $CCCCCO^{\bullet}$ radical (assumption 1, reaction 6′) or from the $CCCCC^{\bullet}OH$ radical (assumption 2, reaction 6) (Scheme 2). In each case, it is supposed to be formed exclusively in the presence of O_2. It will be shown later that only assumption 2 is consistent with our experimental results.

In the case of assumption 1, and taking into account the stationary state approximation, it can be shown that the ratio [pentanal]/[hydroperoxypentanal] is a linear function of the molecular concentration of oxygen, denoted O_2:

$$f(O_2) = \frac{(k_3 + k_9)k'_6(k_2 O_2 + k_{-1})}{k_1 k_2 k_3} \quad (1)$$

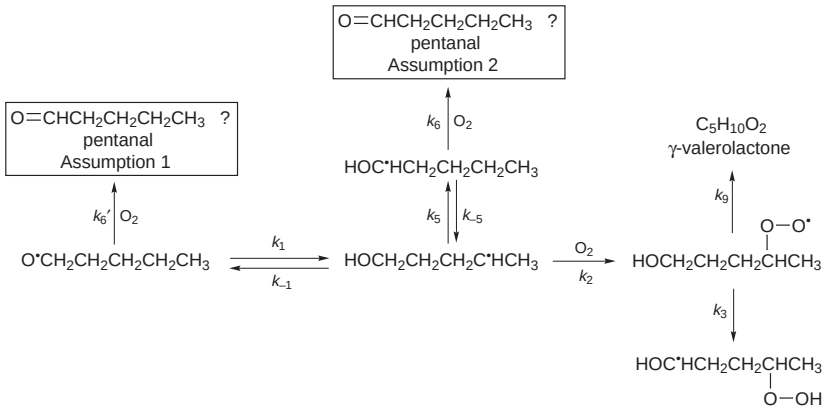

Scheme 2

Fig. 9 shows the experimental values of this ratio. At high concentrations of O_2, eqn. (1) has to explain the flat level experimentally observed ($f_{exp} \approx 0.3$ for concentrations of O_2 higher than 5%). Let us note O_2^{min} and O_2^{max} the limits of the oxygen concentration for which this flat level is observed ($O_2^{min} \approx 8 \times 10^{17}$ mol cm^{-3} and $O_2^{max} \approx 1.6 \times 10^{19}$ mol cm^{-3}): $f(O_2)$ is independent of O_2, for O_2 in the range O_2^{min} to O_2^{max}. The model accounts for experiments if, and only if

$$k_{-1} \gg k_2 O_2^{max} \quad (2)$$

If eqn. (2) is not valid, taking into account the values of k_2 and k_{-1}, then the above model is wrong (it is impossible to obtain a quasi-constant ratio for the O_2^{min}, O_2^{max} concentration range). To refute assumption 1, it is sufficient to show that if eqn. (2) is true then it leads to an abnormal result. Thus $f(O_2)$ indeed becomes, if moreover $k_9 \ll k_3$ [γ-valerolactone] is much lower than [hydroperoxypentanal]:

$$f(O_2) \approx \frac{k'_6 k_{-1}}{k_1 k_2}$$

By using the steady state value determined from the experiments, $f_{exp} \approx 0.3$, we find:

$$\frac{k'_6}{k_2} = f_{exp} \frac{k_1}{k_{-1}} \approx 0.3 \frac{k_1}{k_{-1}} \quad (3)$$

Eqn. (3) is incompatible with the ratios k_1/k_{-1} and k'_6/k_2. The calculated value of the first ratio (k_1/k_{-1}) is 1210 (Thergas software),[28] whereas the second one (k'_6/k_2) must be lower than 0.1. Thus, we have proven that, in the framework of assumption 1, if the model enables one to find a flat level (quasi-constant ratio for the considered O_2 concentration range) it cannot predict its value.

Applying the same type of argument to assumption 2, the ratio [pentanal]/[hydroperoxypentanal] then becomes a decreasing function of the molecular concentration of oxygen:

$$f(O_2) = \frac{(k_3 + k_9)k_5 k_6}{k_2 k_3(k_6 O_2 + k_{-5})} \quad (4)$$

A quasi-constant ratio for $f(O_2)$ can only be found if:

$$k_{-5} \gg k_6 O_2^{max} \quad (5)$$

Eqn. (5) being plausible, the model is able to give a quasi-constant ratio, on the O_2^{min}, O_2^{max} concentration range. Can it predict the flat level numerical value? Taking into account eqn. (5), eqn. (4) becomes, with the approximation that $k_9 \ll k_3$:

$$f(O_2) \approx \frac{k_6 k_5}{k_2 k_{-5}} \quad (6)$$

The measured steady state, $f_{exp} \approx 0.3$, enables us to write:

$$\frac{k_6}{k_2} = f_{exp} \frac{k_{-5}}{k_5} \approx 0.3 \frac{k_{-5}}{k_5} \quad (7)$$

Knowing that $k_5/k_{-5} = 15.7$,[28] eqn. (7) is valid, and we find:

$$k_6 \approx \{(0.3k_2)/15.7\} = 0.019\ k_2$$

In conclusion, we note that only the second assumption (pentanal generated, in presence of O_2, from the CCCCC•OH radical, k_6) enables us to describe the experimental results at high [O_2].

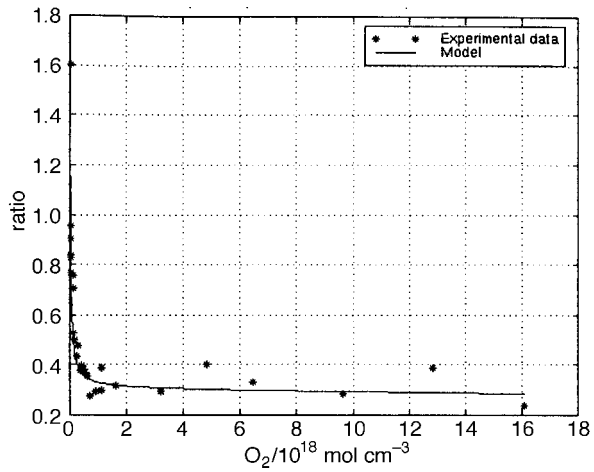

Fig. 9 Experimental data and the analytical steady state for the pentanal/hydroperoxypentanal ratio *versus* O_2 at 473 K

Taking account of heterogeneous reactions

Eqn. (6) gives the ratio [pentanal]/[hydroperoxypentanal] in the case where only the gas-phase reaction is taken into account. This relation, implying a constant ratio in the O_2 concentration range experimentally investigated, is the proof that we have to introduce a heterogeneous reaction (for passivated quartz reactors), so as to take into account the experimental results at low concentrations of oxygen.

We take as a starting assumption that heterogeneous reactions producing pentanal can occur from the CCCCCO• radical (reaction 17), from the CC•CCCOH radical (reaction 13) or from the CCCCC•OH radical (reaction 10). Moreover, we have to introduce reactions producing 2,3-dihydro-5-methylfuran. The two other methylfurans are not taken into account, owing to their low concentration. We thus suppose, as a first assumption, that dihydro-5-methylfuran is exclusively formed by a heterogeneous pathway, and we take as

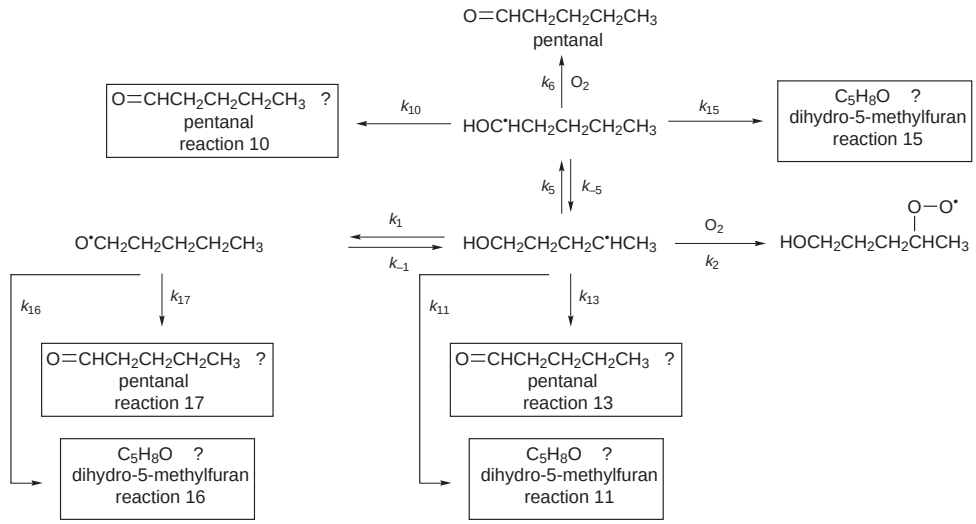

Scheme 3

conceiveable reactions that of the CCCCCO• radical (reaction 16), the CC•CCCOH radical (reaction 11), or the CCCCC•OH radical (reaction 15) (Scheme 3).

Two cases have been investigated. In the first one we assumed that there was no dihydro-5-methylfuran production from the CCCCCO• radical ($k_{16} = 0$). In that case, the steady state analytical solution study revealed unacceptable discrepancies between model and experimental observations. The solution obtained with $k_{16} = 0$ implies that if the ratio pentanal/hydroperoxypentanal is quasi-invariant in the range $[O_2^{min}, O_2^{max}]$ then, necessarily, the ratio (pentanal/dihydro-5-methylfuran) is quasi-linear for $O_2 \leqslant O_2^{max}$, which is evidently not experimentally verified (Fig. 10). As a conclusion of the analytical study, models assuming no dihydro-5-methylfuran production before the first isomerization must be rejected.

In the second case, dihydro-5-methylfuran was supposed to be formed from CCCCCO• ($k_{16} \neq 0$). We also supposed that reactions 11 and 15 could be neglected (production of dihydro-5-methylfuran only through reaction 16), and that there was only one heterogeneous reaction producing pentanal (10, 13 or 17, exclusively). Analysis of a steady state solution did not produce *a priori* incoherences with the experimental results. We therefore moved on to the following step, which consisted of the search for rate constants appearing in this model that give the best prediction of the measured values of the ratios of pentanal/hydroperoxypentanal and pentanal/dihydromethylfuran. To do this we used an optimization method, following a methodology described later in this paper. After a successful analytical solution inspection (already mentioned), a second test was applied to the model: numerical values for the rate constants obtained from the optimization procedure must be physically realistic, according to our knowledge of involved reactions. At this point the model failed: as soon as a heterogeneous reaction (dihydromethylfuran or pentanal, k_{16} or k_{17}, respectively) is supposed to occur from the CCCCCO• radical, its associated rate constant takes a disproportionate value. This result is not surprising; in the contrary case, those reactions would not be able to compete with the first isomerization (reaction 1), which is very fast. As a consequence, every heterogeneous reaction located before the first isomerization can only have a negligible effect on the concentrations of pentanal or dihydro-5-methylfuran as soon as one assigns to that reaction a physically realistic value. But the experimental results clearly show that these heterogeneous reactions are certainly not negligible.

Since none of the working assumptions retained at this stage are satisfactory, we have to introduce a modification in the proposed mechanism. We are going to demonstrate in the following that assuming a homogeneous production of dihydromethylfuran leads to an acceptable model.

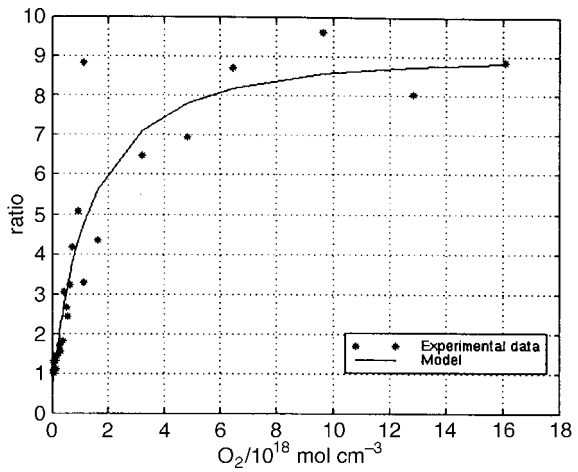

Fig. 10 Experimental data and the analytical steady state for the pentanal/dihydromethylfuran ratio *versus* O_2 at 473 K

Homogeneous formation of dihydromethylfuran

From the similarity of the results concerning pentanal and dihydromethylfuran, it can be thought that they are formed by similar pathways. The ratio, indeed, of one or the other of these two species (with hydroperoxypentanal) is a strongly decreasing function of O_2, for oxygen concentrations lower than 5% (see Fig. 11 and 12). For concentrations higher than 5%, one finds the presence of a flat level in each case. We have already mentioned that, for the ratio pentanal/hydroperoxypentanal, this experimentally observed level is located at *ca.* 0.3. The level of the ratio dihydro-5-methylfuran/hydroperoxypentanal is about eight times lower (0.04), but remains significant. The formation of dihydro-5-methylfuran through an homogeneous pathway, in the presence of O_2, could be an explanation of the fact that this species is still observed, at non-negligible quantities (although these remain low), under high O_2 concentrations.

To locate the homogeneous reaction leading to dihydro-5-methylfuran, we shall adopt the same procedure as for pentanal, by neglecting, as a first approximation, the heterogeneous reactions (this approximation is valid for O_2 concentrations higher than 5%). We shall suppose *a priori* that dihydro-5-methylfuran can be formed from the CCCCCO• radical (assumption 1), from the CC•CCCOH radical (assumption 2) or from the CCCCC•OH radical (assumption 3) (Scheme 4).

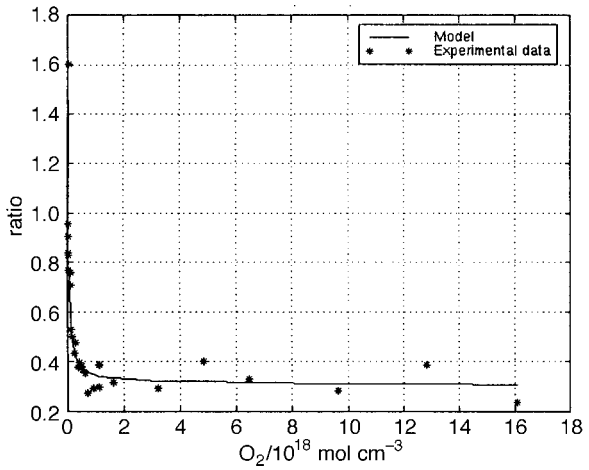

Fig. 11 Experimental data and the numerical solution at time $t = 5$ s for the pentanal/ hydroperoxypentanal ratio *versus* O_2 at 473 K

Before going further, it is advisable to verify that the addition of homogeneous reactions for dihydro-5-methylfuran does not modify the conclusions relative to the homogeneous production of pentanal. If $k_{14} = 0$, eqn. (4) remains unchanged, and the following analysis remains valid. For the contrary case, the expression of the ratio pentanal/ hydroperoxypentanal becomes:

$$f(O_2) = \frac{(k_3 + k_9)k_5 k_6}{k_2 k_3[(k_6 + k_{14})O_2 + k_{-5}]}$$

The quasi-invariance condition of this ratio in the range $[O_2^{min}, O_2^{max}]$ is slightly modified:

$$k_{-5} \gg (k_6 + k_{14})O_2^{max} \quad (8)$$

Nothing being opposed to the verification of this relation, eqn. (6) and (7) are valid in every case.

At present, let us observe the ratio dihydro-5-methylfuran/ hydroperoxypentanal. Within the framework of assumption 1 ($k_{18} \neq 0$, $k_{12} = 0$, $k_{14} = 0$) it can be demonstrated by the same kind of argument used for homogeneous pentanal that the model accounts for the experimentally observed flat level only if:

$$\frac{k_{-1}}{k_2} \gg 2 \times 10^{19}$$

The orders of magnitude of k_{-1} and k_2 from the literature are against the verification of this relation, which leads us to reject assumption 1.

Moving on to assumption 2 ($k_{12} \neq 0$, $k_{14} = 0$, $k_{18} = 0$), it can be shown that the condition to be verified by the rate constants to describe the flat level becomes:

$$\frac{k_{12}}{k_2} \approx 0.04 \quad (9)$$

In the frame of assumption 3 ($k_{14} \neq 0$, $k_{12} = 0$, $k_{18} = 0$), the same analysis leads to:

$$\frac{k_{14}}{k_2} \approx 2.5 \times 10^{-3} \quad (10)$$

by using the calculated value: $k_5/k_{-5} = 15.7$.[28]

Eqn. (9) and (10) being plausible, neither assumptions 2 nor 3 can be excluded at the end of the present analysis.

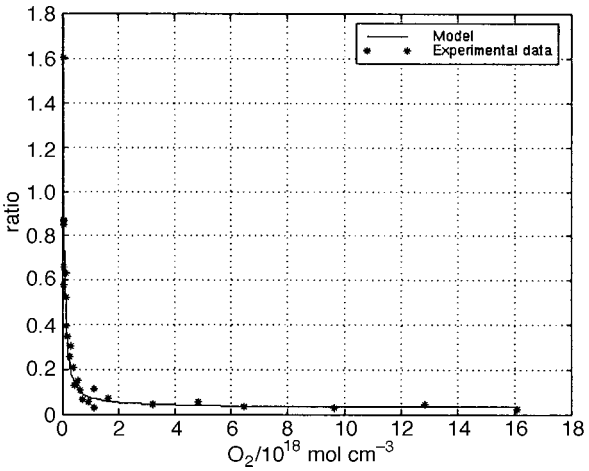

Fig. 12 Experimental data and the numerical solution at time $t = 5$ s for the dihydromethylfuran/hydroperoxypentanal ratio *versus* O_2 at 473 K

Homogeneous and heterogeneous formation of pentanal and dihydro-5-methylfuran

Taking into account what has been concluded about the formation of pentanal and dihydro-5-methylfuran, homogeneously as well as heterogeneously, it remains only to examine the routes represented in Scheme 5: heterogeneous reactions (dihydro-5-methylfuran and pentanal) from the CC˙CCCOH or CCCCC˙OH radicals, homogeneous production of dihydro-5-methylfuran from the same species, and homoge-

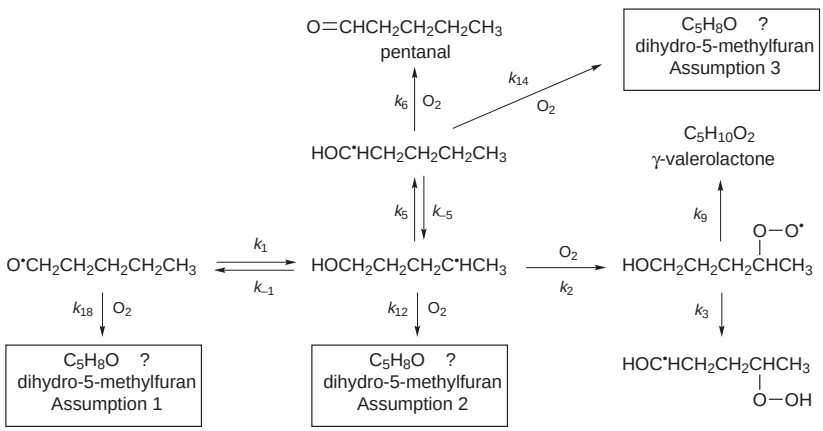

Scheme 4

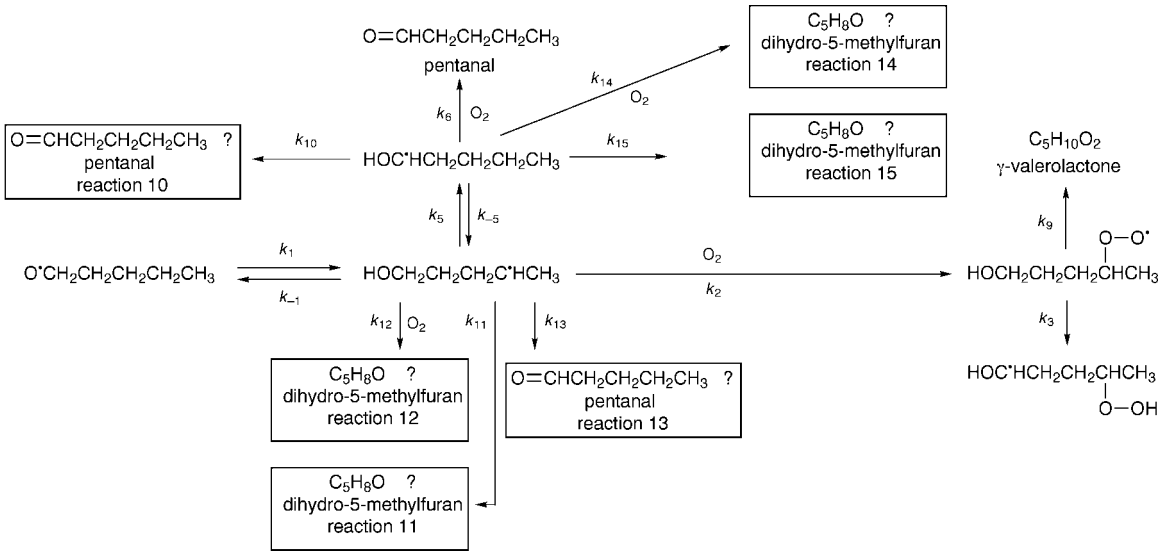

Scheme 5

neous production of pentanal from the CCCCC•OH radical (Scheme 5).

For the model taking into account the whole of these reactions, the analytical expressions of the ratios pentanal/hydroperoxypentanal and pentanal/dihydro-5-methylfuran are, respectively, written as

$$f(O_2) = \frac{b_1 O_2 + b_0}{O_2(a_2 O_2 + 1)} \tag{11}$$

and

$$g(O_2) = \frac{\beta_1 O_2 + \beta_0}{\alpha_2 O_2^2 + \alpha_1 O_2 + 1} \tag{12}$$

The expression of the parameters appearing in these relations is given in the Appendix. In particular, it can be shown from those relations that:

$$\beta_1 = \beta_0 \frac{b_1}{b_0} \tag{13}$$

Eqn. (8) also enables one to establish:

$$(k_6 + k_{14})O_2^{max} \ll k_{-5} \Rightarrow \begin{cases} a_2 O_2^{max} \ll 1 \\ \alpha_2 O_2^{max} \ll \alpha_1 \end{cases} \Rightarrow \begin{cases} a_2 \approx 0 \\ \alpha_2 \approx 0 \end{cases}$$

This enables us to reduce the number of parameters present in eqn. (11) and (12) to, respectively,

$$f(O_2) \approx b_1 + \frac{b_0}{O_2} \tag{14}$$

and

$$g(O_2) \approx \frac{\beta_0(b_1 O_2 + b_0)}{b_0(\alpha_1 O_2 + 1)} \tag{15}$$

Analysis of the functions $f(O_2)$ and $g(O_2)$ does not reveal incoherences with experimental results, thus we can implement the optimization method to identify the rate constants appearing in this mechanism. We look for parameters b_0, b_1, α_1 and β_0, minimizing the sum of the quadratic differences between the calculated and measured values of pentanal/hydroperoxypentanal and pentanal/dihydromethylfuran ratios (minimax problem, solved by the sequential quadratic programming algorithm, Matlab software). All the trials realized with different initial estimates led to the following result:

$$b_0 = 2.6 \times 10^{16} \qquad b_1 = 0.30$$

$$\alpha_1 = 7.0 \times 10^{-19} \qquad \beta_0 = 0.60$$

Fig. 9 and 10 show good agreement between the model and experimental data, the identified values being used for calculation. Subsequently we use b_0, b_1, α_1, β_0 analytical expressions, given in the Appendix, to get the rate constant values. With eqn. (8) and the approximations $k_9 \ll k_3$, $k_{10} \ll k_{-5}$, $k_{15} \ll k_{-5}$, $k_{11} \ll k_5$ we obtain the following set of algebraic equations:

$$b_0 \approx \frac{(k_5 k_{10} + k_{13} k_{-5})}{k_2 k_{-5}} \approx 2.6 \times 10^{16} \tag{16a}$$

$$b_1 \approx \frac{k_6 k_5}{k_2 k_{-5}} \approx 0.30 \tag{16b}$$

$$\alpha_1 \approx \frac{k_5 k_{14} + k_{12} k_{-5}}{k_5 k_{15} + k_{11} k_{-5}} \approx 7.0 \times 10^{-19} \tag{16c}$$

and

$$\beta_0 \approx \frac{k_5 k_{10} + k_{13} k_{-5}}{k_5 k_{15} + k_{11} k_{-5}} \approx 0.60 \tag{16d}$$

By taking $k_5/k_{-5} = 15.7$,[28] we obtain from eqn, (16b):

$$\frac{k_6}{k_2} \approx 0.019 \tag{17}$$

If there is only one heterogeneous pathway for pentanal, and for dihydro-5-methylfuran only one heterogeneous pathway and only one homogeneous pathway, the following ratios are, respectively, obtained from eqn. (16a), (16d) and (16c):

$$\frac{k_{10}}{k_2} \approx 1.7 \times 10^{15} \quad (18a) \qquad \text{or} \qquad \frac{k_{13}}{k_2} \approx 2.6 \times 10^{16} \quad (19a)$$

$$\frac{k_{15}}{k_2} \approx 2.8 \times 10^{15} \quad (18b) \qquad \text{or} \qquad \frac{k_{11}}{k_2} \approx 4.3 \times 10^{16} \quad (19b)$$

$$\frac{k_{14}}{k_2} \approx 1.9 \times 10^{-3} \quad (18c) \qquad \text{or} \qquad \frac{k_{12}}{k_2} \approx 3 \times 10^{-2} \quad (19c)$$

Taking $k_2 \approx 10^{-13}$, we obtain the values summarized in Table 2, in which is also shown the recombination coefficient γ, for the heterogeneous reactions (calculations are performed by considering that heterogeneous reactions occur in the kinetic regime). We want to point out that these proposed rate constant numerical values depend on the choice of k_2, which cannot be deduced from our experiments. All sets of rate constants verifying eqn. (17) to (19) ratios will be in agreement with our experimental results.

Table 2 Proposed set of rate constants numerical values

	homogeneous pentanal	heterogeneous pentanal		homogeneous dihydro-5-methylfuran		heterogeneous dihydro-5-methylfuran	
reaction	6	10	13	14	12	15	11
k	1.9×10^{-15}	170	2600	1.9×10^{-16}	3×10^{-15}	280	4300
γ		5×10^{-3}	8×10^{-2}			8×10^{-3}	0.13

We must now decide which pathways lead to pentanal and dihydro-5-methylfuran formation. All possibilities being open, we keep in mind that heterogeneous pentanal is produced from the same radical as the homogeneous pentanal, *i.e.* the CCCCC˙OH radical (reaction 10). The position, indeed, of the free bond should promote the formation of the C=O double bond. It is a similar reason which leads us to think that dihydro-5-methylfuran would, at the opposite, be formed from CC˙CCCOH radical (reactions 11 and 12). The free bond position could, indeed, favour the formation of these cyclic species. These assumptions are retained for the numerical simulation presented below. The proposed mechanism is in Scheme 6.

Remarks. Among the compounds observed during our experiments and identified, pentan-1-ol is listed. This alcohol, as it was the case for butan-1-ol which was formed in the *n*-butoxy/O_2 system,[7] is not taken into account in the general mechanism.

During our investigations, we could not observe a decomposition route for the *n*-pentoxy radical. Several species containing four carbons in their formula could be detected, but their concentration is so low that even at a higher temperature (523 K) it was impossible to undertake a specific study of this pathway. This decomposition route appears on the chemical mechanism, but its location is made by analogy with other alkoxy radicals.

Numerical simulation

The differential equations system ensuing from the proposed mechanism is numerically solved according to 'Numerical Differentiation Formulas.' This resolution mode enables us to be free of the stationary state assumption and also from the approximations made.

For the simulation, we have chosen the rate constant values summarized in Table 3. The results at time $t = 5$ s are given in Fig. 11, 12 and 13 for the ratios pentanal/hydroperoxypentanal, dihydromethylfuran/hydroperoxypentanal and γ-valerolactone/hydroperoxypentanal, respectively. Good agreement between calculations and the experimental data

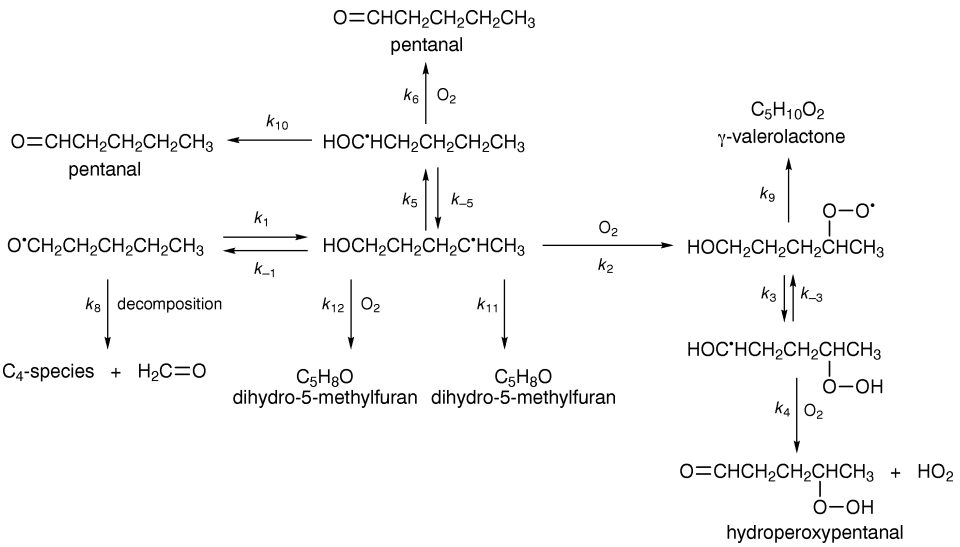

Scheme 6

Table 3 Rate constants k and heterogeneous recombination coefficients γ used for the numerical simulation[a]

reaction	k	γ	A	E_a		ref.
0	0.1		10^{16}	37.0		29
1	3.8×10^{8}		8.4×10^{10}	5.1		27
−1	3.1×10^{5}				$k_1/k_{-1} = 1210$	28
2	10^{-13}					this work
3	1151		6.4×10^{10}	16.9		23
−3	2.4×10^{5}		2.4×10^{9}	8.7		24
4	2.7×10^{-12}		1.2×10^{-10}	1.8		26
5	1.57×10^{7}				$k_5/k_{-5} = 15.7$	28
−5	10^{6}				from eqn. (5): $k_{-5} \gg 3 \times 10^{4}$	this work
6	1.9×10^{-15}					this work
8	7.5×10^{6}		8×10^{14}	17.4		30
9	71	2×10^{-3}				this work
10	170	5×10^{-3}				this work
11	4300	0.13				this work
12	3×10^{-15}					this work

[a] k, rate constant in molecules cm^{-1} s^{-1}; preexponential factor A; activation energy E_a (kcal mol^{-1}); γ, recombination coefficient; temperature = 473 K.

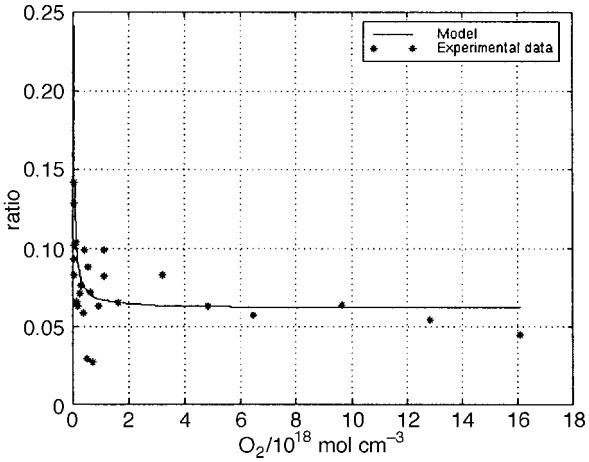

Fig. 13 Experimental data and the numerical solution at time $t = 5$ s for the γ-valerolactone/hydroperoxypentanal ratio *versus* O_2 at 473 K

supports the approximations needed to build up the chemical mechanism. In particular, the observation of results at different instants shows that we have to go down to residence times of about 10 ms to notice a time dependence of the concentration ratios. Throughout the experiments the residence time was never lower than 1 s.

Conclusions

A systematic investigation of the homogeneous and heterogeneous reactions of n-$C_5H_{11}O$, n-$C_5H_{10}OH$ and $OOC_5H_{10}OH$ radicals in oxygen was performed at temperatures near 473 K. Different reactors and a great variety of O_2 concentrations (O_2 percentage ranging from ~0 to 100%) were used. Experimental data were used to set up a chemical mechanism and to evaluate rate constants. An analytical solution was found by using the Laplace transform, and the corresponding rate constants were evaluated by an optimization method.

It could be shown that:†

pentanal and methylfurans are formed in the gas phase after isomerization of RO˙ radicals;

pentanal and methylfurans are also heterogeneously formed (especially at low oxygen concentrations, <5% O_2), this production occurring from the same isomerized radical as in the gas phase, *i.e.* from the CCCCC˙OH radical for pentanal and from the CC˙CCCOH radical for methylfurans;

γ-valerolactone is heterogeneously produced from $HOR_{-H}OO$ radicals;

pentanal-hydroperoxide, $O{=}CH(CH_2)_2CH(OOH)CH_3$, is formed in the gas phase after a second isomerization, $OOR_{-H}OH \rightarrow HOOR_{-2H}OH$.

All these reactions are to be taken into account in connection with pollution in the presence of dust or ash in the atmosphere or under urban conditions.

The heterogeneous reaction of $HOR_{-H}OO$ radicals is much slower than that of $R_{-H}OH$ radicals. But, as the gas-phase reaction of $HOR_{-H}OO$ radicals is slow, this heterogeneous reaction might play an important role. Specific investigations are needed to determine the influence of diffusion, towards the walls, in comparison with heterogeneous reactions: under anticyclonic calm conditions, diffusion plays a role over several cm and heterogeneous reactions would be negligible; but, the presence of a draught could make these reactions significant, because they would act as a radical sink. Under those conditions, diffusion should still play its part.

† The isomerization reaction of RO˙ radicals is fast; for this reason, direct reactions from RO˙ radicals, as well homogeneous (with O_2) and heterogeneous reactions are negligible. In internal combustion engines with direct injection, spark-ignition or diesel, the reactions of RO˙ and RO_2˙ radicals can be significant: near the walls, in the presence of liquid, identical compounds were found.[31]

Appendix

Analytical solution of the stationary state

$$a_2 = \frac{k_6 + k_{14}}{C}$$

$$b_0 = \frac{(k_3 + k_9)(k_5 k_{10} + k_{13} C)}{k_2 k_3 C}$$

$$b_1 = \frac{(k_3 + k_9)[k_5 k_6 + k_{13}(k_6 + k_{14})]}{k_2 k_3 C}$$

$$\alpha_1 = \frac{k_5 k_{14} + k_{11}(k_6 + k_{14}) + k_{12} C}{k_5 k_{15} + k_{11} C}$$

$$\alpha_2 = \frac{k_{12}(k_6 + k_{14})}{k_5 k_{15} + k_{11} C}$$

$$\beta_0 = \frac{k_5 k_{10} + k_{13} C}{k_5 k_{15} + k_{11} C}$$

$$\beta_1 = \frac{k_5 k_6 + k_{13}(k_6 + k_{14})}{k_5 k_{15} + k_{11} C}$$

with: $C = k_{-5} + k_{10} + k_{15}$

NB: reaction −3 is neglected in the analytical calculation.

References

1 K. Sahetchian, J. C. Champoussin, M. Brun, N. Levy, N. Blin-Simiand, C. Aligrot, F. Jorand, M. Socoliuc, A. Heiss and N. Guerrassi, *Combust. Flame*, 1995, **103**, 207; B. S. Haynes and H. Gg Wagner, *Proc. Energy Combust. Sci.*, 1981, **7**, 229; R. J. Price, J. P. T. Wilkinson, D. A. I. Jones and C. Morley, *SAE Technical Paper Series* 952445; G. T. Kalghatgi, *SAE Technical Paper Series* 952443.

2 C. Kim, Sh. W. S. Cheng and Sh. A. Majorski, *SAE Technical Paper Series* 912379.

3 N. Blin-Simiand, F. Jorand, K. Keller, M. Fiderer and K. Sahetchian, *Combust. Flame*, 1998, **112**, 278.

4 D. Gutman, N. Sanders, and J. E. Butler, *J. Phys. Chem.*, 1982, **86**, 66; P. J. Wantuck, R. C. Oldenborg, S. L. Baughcum and K. R. Winn, *J. Phys. Chem.*, 1987, **91**, 4653.

5 D. Gutman, N. Sanders and J. E. Butler, *J. Phys. Chem.*, 1982, **86**, 66; K. Lorenz, D. Rhäsa, R. Zellner and B. Fritz, *Ber. Bunsen-ges. Phys. Chem.*, 1985, **89**, 341; D. Hartmann, J. Karthäuser, J. P. Sawerysyn and R. Zellner, *Ber. Bunsen-ges. Phys. Chem.*, 1990, **94**, 639.

6 R. J. Balla, H. H. Nelson and J. R. McDonald, *Chem. Phys.*, 1985, **99**, 323.

7 A. Heiss and K. Sahetchian, *Int. J. Chem. Kinet.*, 1996, **28**, 531.

8 F. Jorand, A. Heiss, K. Sahetchian, L. Kerhoas and J. Einhorn, *J. Chem. Soc., Faraday Trans.*, 1996, **92**, 4167.

9 J. E. Eberhard, C. Muller, D. W. Stocker and J. A. Kerr, *Environ. Sci. Technol.*, 1995 **29**, 232.

10 R. Atkinson, E. S. C. Kwok, J. Arey and S. M. Aschmann, *Faraday Discuss.*, 1995, **100**, 23.

11 R. Atkinson and S. M. Aschmann, *Environ. Sci. Technol.*, 1995, **29**, 528.

12 E. S. C. Kwok, J. Arey and R. Atkinson, *J. Phys. Chem.*, 1996, **100**, 214.

13 S. Dobé, T. Bérces and F. Marta, *Int. J. Chem. Kinet.*, 1986, **18**, 329.

14 P. Gray, R. Shaw and J. C. J. Thynne, *Progress in Reaction Kinetics*, Pergamon Press, Oxford, 1967, vol. 4, p. 63.

15 L. Batt, *Int. Rev. Phys. Chem.*, 1987, **6**, 53.

16 W. P. L. Carter, K. R. Darnall, A. C. Lloyd, A. M. Winer and J. N. Pitts, *Chem. Phys. Lett*., 1976, **42**, 22; W. P. L. Carter, A. C. Lloyd, J. L. Sprung and J. N. Pitts, *Int. J. Chem. Kinet*., 1979, **11**, 45.
17 A. C. Baldwin, J. R. Barker, D. M. Golden and D. G. Hendry, *J. Phys. Chem*., 1977, **81**, 2483.
18 W. P. L. Carter, J. A. Pierce, D. Luo and I. L. Malkina, *Atmos. Environ*., 1995, **29**, 2499.
19 W. P. L. Carter, R. Atkinson, A. M. Winer and J. N. Pitts, *Int. J. Chem. Kinet*., 1982, **14**, 1071.
20 J. P. Killus and G. Z. Whitten, *Int. J. Chem. Kinet*., 1990, **22**, 547.
21 V. Mörs, A. Hoffmann, W. Malms and R. Zellner, *Air Pollut. Res. Rep*., 1996, **57**, 273.
22 T. P. W. Jungkamp, J. N. Smith and J. H. Seinfeld, *J. Phys. Chem. A*, 1997, **101**, 4392.
23 O. Perrin, A. Heiss, K. Sahetchian, L. Kerhoas and J. Einhorn, *Int. J. Chem. Kinet*., in press.
24 E. R. Ritter and J. W. Bozzelli, *Int. J. Chem. Kinet*., 1991, **23**, 767; J. W. Bozzelli and W. J. Pitz, *Twenty-fifth Symposium (International) on Combustion*, The Combustion Institute, Pittsburgh, PA, 1994, p. 783.
25 F. Welch, H. R. Williams and M. S. Mosher, *J. Am. Chem. Soc*., 1955, **77**, 551.
26 D. L. Baulch, C. J. Cobos, R. A. Cox, C. Esser, P. Frank, Th. Just, J. A. Kerr, M. J. Pilling, J. Troe, R. W. Walker and J. Warnatz, *J. Phys. Chem. Ref. Data*, 1992, **21**, 686.
27 R. Atkinson, *Atmos. Environ*., *A*, 1990, **24**, 1.
28 C. Muller, V. Warth, E. Jacquemard, G. Scacchi and G. M. Côme, *Software THERGAS*, ENSIC-INPL and Université de Nancy I.
29 K. Sahetchian, R. Rigny, N. Blin and A. Heiss, *J. Chem. Soc., Faraday Trans. 2*, 1987, **83**, 2035.
30 A. P. Altshuller, *J. Atmos. Chem*., 1991, **12**, 19.
31 N. Blin-Simiand, F. Jorand, M. Brun and K. Sahetchian, *Combust. Sci. Technol*., submitted.

Paper 8/03340D; *Received* 5*th May*, 1998